POLITECNICO
MILANO 1863

SCUOLA DI INGEGNERIA INDUSTRIALE
E DELL'INFORMAZIONE

Executive Summary of the Thesis

Aerogel-based collection of ejecta material from asteroids from Libration point orbits: dynamics and capture design

Laurea Magistrale in Space Engineering - Ingegneria Spaziale

Author: Carlo Burattini

Advisor: Prof. Camilla Colombo

Co-advisor: Mirko Trisolini

Academic year: 2022-2023

1. Introduction

Asteroids are thought to provide important hints on the early Solar System and, not less important, they could represent a valuable source of metals, silicates and water. Several missions, such as Deep Impact (NASA), OSIRIS-REx (NASA), Hayabusa and Hayabusa2 (JAXA), in the past few years carried on efforts aimed to improve and better identifying the main properties of these yet poorly known celestial bodies. Moreover, these celestial bodies grant also the possibility to conduct space exploration at reasonable costs, representing therefore the perfect targets for the next space achievements. With this in mind, it is straightforward to understand how important would be to successfully gather asteroids samples without neither landing on them. This work, in fact, aims to understand the feasibility of a collection mission through a satellite orbiting around the second Libration point. Assessing this, would be of huge importance since not only it would prevent any complication related to touchdown maneuvers, but also it would avoid all the dead times present in a landing mission. In this case, the reference scenario is the one of the asteroid Ryugu, whose main properties are given in Table 1.

Property	Value
Effective Radius	440 m
Ellipsoid Axis	$a = 446.5$ m $b = 439.7$ m $c = 433.9$ m
μ_a	$32 m^3/s^2$
Density (Bulk)	1282 kg/m^3

Table 1: Main properties of Ryugu.

2. Dynamical Model and Equations

Being involved in the study of Sun-Ryugu system implies, of course, to investigate the motion of asteroid ejecta within the Three-Body Problem. Indicating with m_S, m_R and $m_{S/C}$ the masses of Sun, Ryugu and spacecraft respectively, it will hold that $m_S > m_R >> m_{S/C}$, meaning that the third body can be considered as a "mass-less" object that cannot affect the motion of the other bodies. With this consideration, and assuming also that the primaries follow circular paths, it is possible to reduce the problem to the Circular Restricted Three Body Problem (CR3BP). However, it is much more convenient to work with autonomous systems, which do not depend explicitly on time. The biggest advantage arising from this is that all the

features investigated through this approach will be valid at any time instant. To reach this goal, it is possible to translate the problem into the synodic frame, rotating in the x-y plane with the same angular rate of the system: the position of the two primaries remains therefore fixed with respect to its origin. Furthermore, typically the problem is adimensionalised, in order to work with non-dimensional quantities, thus improving the efficiency and accuracy of computational and numerical methods applied. Taking:

- the reference mass equal to $M_{ref} = m_S + m_R$;
- the reference length equal to the Sun-Ryugu distance, i.e. $l_{ref} = 1.19$ AU;
- the time unit τ driving to a unit angular rate ($\Omega = 1$).

The discussion done until now does not include any perturbation affecting the motion of the third body. However, in general, this is not true. In particular, referring to Gustafson [1], with s being the linear dimension of a particle, while gravity is proportional to s^3 and pressure forces to s^2, electromagnetic Lorentz forces are proportional to s, which can usually be neglected for micrometer-sized particles. For these reasons, the disturbances considered will be the ones due to the solar radiation and the aspherical harmonics gravitational perturbation.

The effect of solar radiation pressure (SRP) is considered through a cannon-ball model, enabling to treat its force as conservative. The key parameter is the lightness parameter β, which can be defined as the ratio between the SRP acceleration and the solar gravity acceleration, obtained therefore through Equation 1, where AU is the astronomic units ($= 1.496 \cdot 10^8$ km), P_0 is the solar flux at 1AU ($= 1367$ W/m^2), c_R is the particle reflectivity coefficient, ρ_p is the particle density, d_p is the particle diameter.

$$\beta = P_0 \frac{AU^2}{\mu_{sun}} \frac{3c_R}{2\rho_p d_p} \tag{1}$$

Concerning the aspherical potential perturbation, instead, the standard tool used to described it is the spherical harmonics expansion: since it models the distribution of mass inside a sphere circumscribing the body, the method is suitable to describe small deviations from a spherical shape. However, J_2 can be recovered from Ryugu's mean radius and its axis (reported in Table 1) and in this case it is found to be $J_2 = 0.008347066115702$. Taking into account these effects, the equations of motions become those expressed in the equation below where $\mu = m_R/M_{ref}$, $\bar{a} = R_{Ryu}/l_{ref}$, $\bar{n}^2 = 1 + (3/2)J_2\bar{a}^2$, while the terms r_{sp} and r_{ap}, representing the Sun-Particle and Ryugu-Particle distances respectively, can be computed as $r_{sp} = ((x+\mu)^2 + y^2 + z^2)^{1/2}$ and $r_{ap} = ((x+\mu-1)^2 + y^2 + z^2)^{1/2}$. These underline how, whenever considering the SRP, i.e. $\beta \neq 0$, the dynamics of a particle will be strongly dependent on its dimensions, meaning that SRP can be used a passive in-situ mass spectrometer (the larger the grain, the lower the β). Alternatively, after a grinding process to reduce all materials to a similar grain size, SRP can be exploited to sort particles by their density. Such opportunities are crucial to assess the dimensions and properties of the particles that will be gathered in a collection mission.

$$\begin{cases} \ddot{x} - 2\bar{n}\dot{y} = \bar{n}^2 x - \frac{(1-\beta)(1-\mu)(x+\mu)}{r_{sp}^3} - \frac{\mu}{r_{ap}^3}\left[1 - \frac{3}{2}J_2\left(\frac{\bar{a}}{r_{ap}}\right)^2\left(5\frac{z^2}{r_{ap}^2} - 1\right)\right](x+\mu-1) \\ \ddot{y} + 2\bar{n}\dot{x} = \bar{n}^2 y - \frac{(1-\beta)(1-\mu)}{r_{sp}^3} y - \frac{\mu}{r_{ap}^3}\left[1 - \frac{3}{2}J_2\left(\frac{\bar{a}}{r_{ap}}\right)^2\left(5\frac{z^2}{r_{ap}^2} - 1\right)\right] y \\ \ddot{z} = -\frac{(1-\beta)(1-\mu)}{r_{sp}^3} z - \frac{\mu}{r_{ap}^3}\left[1 - \frac{3}{2}J_2\left(\frac{\bar{a}}{r_{ap}}\right)^2\left(5\frac{z^2}{r_{ap}^2} - 3\right)\right] z \end{cases}$$

3. Jacobi Consant and Lagrangian Points

Within the dynamics introduced, it is possible to define the Jacobi constant C, a quantity conserved in time and through the motion of the particle, defining the only integral of motion of the system. By definition, it is half and opposite in sign with respect to the total energy of the system, being defined as $E = (1/2)v^2 + U = -(1/2)C$, being v and U the velocity and the potential respectively. Although the CR3BP cannot be solved in closed form since C is the only conserved quantity, the Jacobi constant is important not only as computational check, but mainly because it can be used to bound the motion of the mass within a prescribed region, defining the Zero Velocity Curve (ZVC). Imposing, in fact, $v = 0$ in the constant's definition, the possible natural motion is bounded within a space region that must solve $C = -2U$. Specifically, an object will be able to move inside the ZVC but never to go outside it (or vice versa)

since it will arrive on this surface with null velocity. In particular, defining a critical Jacobi constant $C^* = -2U$, the forbidden regions will be all those with $C \geq C^*$, since this leads to $v^2 < 0$ that is physically unfeasible. Another piece of information that comes out of writing the problem in the synodic frame is related to the existence of five equilibrium points fixed relatively to the rotating line linking the primaries of the system: in these points, in fact, centrifugal and gravitational forces are balanced. They can be divided into the collinear points, which are three unstable equilibrium points (L_1, L_2, L_3) all located along the line connecting the primaries, i.e. the x-axis; and the equilateral points, two points of stable equilibrium called L_4 and L_5. While these lasts lie on the vertex of equilateral triangles whose base is the segment linking the two primaries (L_4 60° ahead with respect to Ryugu, L_5 60° behind it), the collinear points can be found solving quintic expressions provided by Koon et al. [2]. Once defined the lagrangian points this way, it is possible to investigate how their position, and consequently also the ZVCs, will change when considering the perturbations previously introduced. In particular, it is found out that, for higher values of β, L_2 moves towards the Ryugu while L_1 and L_3 approach the Sun. This is reflected also in the effects linked to J_2, that will be therefore more pronounced at L_2 than at L_1 which, moving towards the Sun, will feel a lower and lower J_2 perturbation. From these considerations it is possible to define the size range of particles that the proposed mission will have interest on. In fact, if L_2 gets closer to Ryugu for higher β, i.e. smaller particles, there will be a value for which it can be found on the asteroid's surface. It is therefore useful to impose a lower limit to the particle size to provide to the ejecta a closed region in the neighborhood of the asteroid within which they can freely move. Fixing a distance of 3 km from Ryugu, it is obtained $\beta = 8.02315 \cdot 10^4$, corresponding to a particle size $r_P \simeq 78.5\ \mu m$. Contrarily, there is no upper limit defined by the physics of the problem. This is then assessed by imposing a maximum size for asteroid ejecta equal to $r_P = 10$ mm, i.e. $\beta = 6.29804 \cdot 10^6$. These limiting cases are shown in Figure 1.

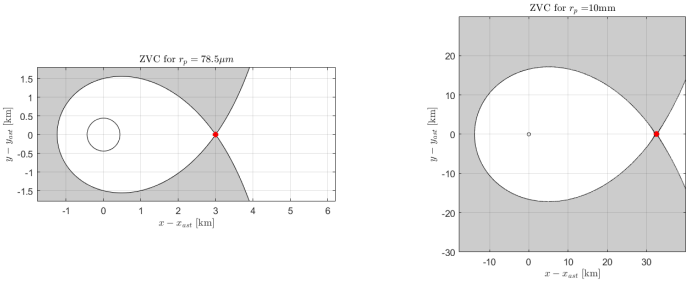

Figure 1: ZVC for $r_P = 78.5\ \mu m$ (left) and $r_P = 10$ mm (right), locating the LP in order at 3 km and 32.48 km from Ryugu.

4. Database Creation

Due to the presence of the integral of motion, if the position and the energy level are fixed, then the velocity is unequivocally determined as well. This allows to exploit an energetic approach to find its value which, from the definition of the Jacobi constant, it is possible to compute with respect to a prescribed energy level: to enlarge the portion of space of interest from just the lagrangian point to a suitable halo region, it has been chosen equal to $C' = 0.9999999999997C_2$ [1]. The choice of such a value shows how sensitive this problem really is and has been imposed taking care of how the ZVC will be affected by it. The new ZVC, in fact, shall still present a shape giving important hints on the direction from where the particles are escaping, both for $r_P = 10$ mm and $r_P = 78.5\ \mu m$. The ejection velocity, therefore, can be recovered, considering also the asteroid's rotation contribute, as expressed in Equation 2, being ω_{rot} and ω_{rev} Ryugu's angular rate around its axis and around the Sun respectively.

$$v_{ej} = \sqrt{C(x, y, \beta) - (\frac{\omega_{rot}}{\omega_{rev}} r_{Ryu})^2 - C'} \qquad (2)$$

The equations of motion are integrated until when the particle hits again the surface of Ryugu or whenever it goes outside the Hill's sphere, i.e. whenever $r_{Ryu} \leq r \leq r_{Hill} = (\mu/3)^{1/3}$. While in the second case the iteration just stops and the next one begins, in all the cases of impacts on Ryugu the bouncing behavior shall be analysed. This is achieved by means of the coefficients of

[1] C_2 is the energetic level of the second lagrangian point.

restitution, defined as the ratios between the velocity before and after the collision, for both normal (e_n) and tangential (e_t) directions. Specifically, these are obtained for each impact angle through an interpolation done on the data provided by Kikuchi et al. [3], analysing both rigid body (RB) and point mass (PM) models, which present different ranges of suitable impact angles driving to a rebound. Specifically, PM is more conservative since it does not requires the limiting rigid body assumption. Moreover, [3] provides data for two different sites on Ryugu, identified here on as TDM1 and TDM2, being in order representative of surface and sub-surface material. Restitution coefficients can be then used to recover the velocity of an ejecta after its impact with Ryugu (see Equation 3) and, once computed it, the particle will be considered to be entered back in orbit only if $(v'_{tn}(2))^2/(2g) > l_{threshold}$, being $l_{threshold}$ a tolerance set equal to 10 cm. If this is the case, post-impact velocity $\boldsymbol{v'_{tn}}$ is rotated back to the inertial frame providing a new initial conditions, otherwise the ejecta can be assumed as touched-down on the asteroid and the next iteration starts.

$$\boldsymbol{v'_{tn}} = \begin{bmatrix} e_t & 0 & 0 \\ 0 & -e_n & 0 \\ 0 & 0 & -1 \end{bmatrix} \boldsymbol{v_{tn}} \tag{3}$$

The whole procedure described is iterated by means of three nested cycles, having $78.5\mu m \leq r_P \leq 10mm$, $0° \leq \theta \leq 360°$ and γ, i.e. the angle between v_{ej} and the local normal, $\in [-65°, -25°] \cup [25°, 65°]$ [4]. The results are then stored in a table having nine columns, forming in this way a database describing the ejecta dynamics and fate: this will enable not only to manage easily the information found but also gives the opportunity to "search" for specific initial conditions and directly recover the final situation without any further process or integration. The columns are $r_P, \theta, v_{ej}, \gamma, \theta_{imp}, v_{imp}, \gamma_{imp}, tof$ (time of flight) and the last one presents the *Condition*, which can be: 1) *Escape*, the ejecta particle has been able to escape from the system; 2) *Impact*, the ejecta particle hit again on Ryugu's surface, with an impact angle within the feasible range; 3) *OutRange*, the ejecta particle hit again on Ryugu's surface, with an impact angle outside the feasible range. The particle here is considered as landed on the surface, unable to bounce back into orbit; 4) *Orbit*, in this case the time of flight is equal to the maximum time window provided (90 days): the ejecta is assumed to be still in orbit around Ryugu; 5) $Escape_{reb}$, same of 1 but after a previous collision with Ryugu and consequent rebound; 6) $Impact_{reb}$, same of 2 but after a previous collision with Ryugu and consequent rebound; 7) $OutRange_{reb}$, same of 3 but after a previous collision with Ryugu and consequent rebound; 8) $Orbit_{reb}$, same of 4 but after a previous collision with Ryugu and consequent rebound. Comparing the results obtained through the method applied by Latino et al. in [5], which considered e_t and e_n as constants equal to 0.714 and 0.6, it is straightforward to understand the necessity of introducing a new model such as the one here proposed, based on the interpolation of the data provided by [3]. Apart from the fact that now the coefficients are no longer constants, which is a strong and unlikely assumption, with the older approach about the 98% of trajectories in $Impact_{reb}$ drives to an orbit after a second rebound, underlining how the damping assumed in this scenario is not realistic.

5. Neck Region Trajectory

Aiming to expand the portion of space of interest from just the libration point to its neighboring zones, it will be necessary to analyse the motion in the neck region. Following Koon et al. [2], it is possible, starting from the linearised lagrangian equations of motion, to retrieve the so-called Lyapunov orbit: this periodic orbit projects onto the xy-plane as an ellipse centered at L2, having major and minor axis of length equal to $2\tau\sqrt{\epsilon/k}$ and $2\sqrt{\epsilon/k}$ respectively, being ϵ a variable ruling the amplitude and k a constant that can be computed as $k = -a + b\tau^2 + \nu^2 + \nu^2\tau^2$, where $\bar{\mu} = \mu|x_e - 1 + \mu|^{-3} + (1-\mu)|x_e + \mu|^{-3}$, $a = 2\bar{\mu} + 1$, $b = \bar{\mu} - 1$ and $\tau = -(\nu^2 + a)/(2\nu)$. Assuming for $r_P = 78.5\ \mu m$ and $r_P = 10$ mm a semi-major axis (SMA) of 0.75 km and 28.5 km respectively, it is possible to retrieve the adimensional values of ϵ as $\epsilon = (SMA_{adim}/\tau)^2 k$, finally obtaining the neck periodic orbits shown in Figure 2.
In the case of $r_P = 78.5\ \mu m$, the small orbit enables the spacecraft to fast "survey" around the whole bottleneck opened: almost all the ejecta escaping through the bottleneck having

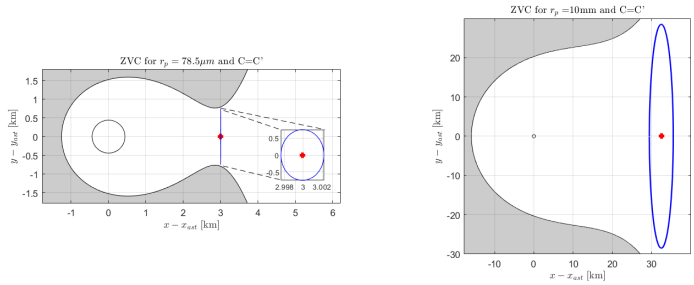

Figure 2: Periodic orbit in the neck region formed by the ZVC with $C = C'$ for $r_P = 78.5\ \mu m$ (left) and $r_P = 10$ mm (right).

sizes close 78.5 μm can be therefore assumed to be captured. Contrarily, the biggest particles will not have to pass through that same aperture, meaning that just a tiny portion of this kind of ejecta can be considered to be actually gathered. On the other hand, the bigger orbit obtained for $r_P = 10$ mm enables the capture of a wider range of particles. In fact, pretty much all the ejecta escaping from the system will pass throughout that portion of space. However, since the orbit is much larger, it can not be ensured that, when an ejecta is escaping, the spacecraft will be there and not in another tract of its path.

6. Results

Firstly, it is interesting to understand the number of particles falling within each category, shown in Figure 3 both for PM and RB.

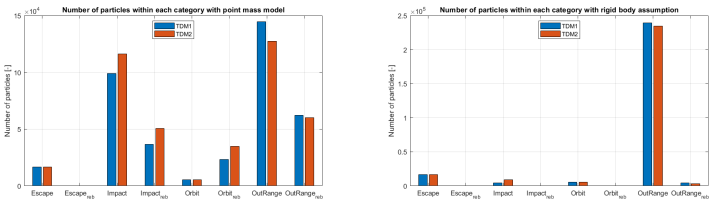

Figure 3: Histogram of the number of ejecta falling within each category for PM (left) and RB (right) models.

It can be noticed from the figure that the number of particles escaping the system does not change when considering PM or RB approximation, remaining equal to 16610 for both TDM1 and TDM2: this is simply explained since the real difference between PM and RB models is the actual range of suitable impact angles. From this consideration it is straightforward to understand that, whatever the chosen approach, it will not affect the behavior of particles that do not impact back on Ryugu, neither for *Escape* nor *Orbit* categories, which counts 5588 ejecta. Contrarily, changing the model will of course result in a drastic change in the number of the ejecta categorized as *OutRange*. Finally, a consideration on the category $Escape_{reb}$: no particle is found to be able to escape from the system after a previous rebound. The trivial indication is that if a particle is ejected with conditions that do not permit a direct escape, that particle will never be able to leave the system neither after a sort of "re-tuning" of its initial conditions by means of an impact: this, of course, is a consequence of the energy dissipation occurring within any collision. However, since the differences between TDM1 and TDM2 are found to be low, from here on just the TDM1 case will be shown due to its representation of the surface material, the one of interest in this work. Furthermore, due to its more conservative formulation, the PM model will be the baseline of the discussion even though RB could represent a better approximation of a real scenario. Focusing now on the escaped ejecta, these are the ones that really rule the feasibility of the mission: Figure 4 reports two contour plots investigating the number of escaping trajectories with respect to r_P, θ and v_{ej}.

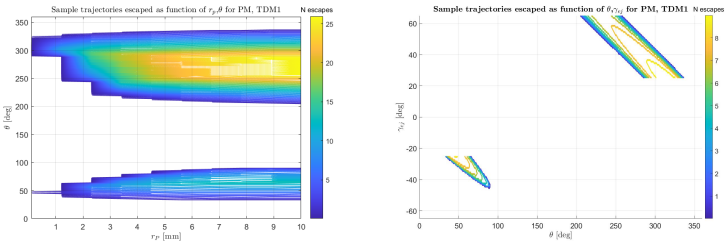

Figure 4: Contour plot on the escaping sample trajectories depending on r_P, θ (left) and on θ, γ_{ej} (right).

The figure on the left shows that the conditions that make a particle able to escape can be divided in two groups: one having $\theta < 100°$ and another with $200° < \theta < 350°$. Moreover, higher r_P lead to a wider θ-range enabling particle escape, driving thus to more escapes. It is possible to conclude that the majority of the ejecta leaving Ryugu will come from the upper group

while no escapes are found for $100° < \theta < 200°$. The plot on the right, instead, shows that for the first group most of the escaping orbits comes from the lowest θ and the highest γ_{ej} while, as θ increases, the escapes are less and require lower γ_{ej}. Contrarily, the other group exhibits the opposite trend: the number of escaped orbits is in fact higher for lower γ_{ej} and increases with θ. This is of course a consequence of the geometry of the problem, highlighting as the conditions maximising escape probability those driving the particle to be ejected directly towards the bottleneck. The other crucial parameter to assess this collection's feasibility is the time window required by the mission. Specifically, choosing as threshold value of the gathered mass the same mass collected on Hayabusa2 mission, i.e. about 5.262 g, it is possible to obtain a preliminary hint on the required time span. Considering the case of a satellite orbiting the left trajectory of Figure 2, chosen to maximise the capture probability, it is possible to gather the required mass just with $r_P \leq 2.283$ mm. The study revealed that, in this scenario, the satellite is able to collect 1.8040 g and 3.458 g for ejecta with $r_P = 1.181$ mm and $r_P = 2.283$ mm respectively. Therefore, since to lower r_P corresponds a slower dynamics, the dominant time-scale will be the one necessary to collect the needed ejecta having $r_P = 2.283$ mm, which, approximating the ejection time with the time the particle takes to leave the Hill's sphere, is found out to be 22.48 days (i.e. 23 days). The other piece of information that is important to understand the collection behavior is the capture velocity, which will be assumed to be the velocity with which the particle run away from the Hill's sphere. Actually, to this purpose, the velocity that should be considered is the relative speed between the ejecta and the spacecraft but, for a preliminary design, the assumption explained before has been retained satisfying. From Figure 5 it is clear that for lower r_P, $V_{capture}$ increases. This is a positive aspect since, otherwise, the kinetic energy would grow with both, likely touching prohibitive values. Furthermore, since higher r_P means higher v_{ej}, particles departing from Ryugu with the highest velocities are the same that could be collected at a lower $V_{capture}$.
To conclude, apart for some isolated case, almost all the particles will have 100 m/s $\leq V_{capture} \leq$ 300 m/s, with the maximum kinetic energy corresponding to $E_{max} = 1.9258 \cdot 10^{-4}$ J. This value will be particularly important for the capture mechanism's design.

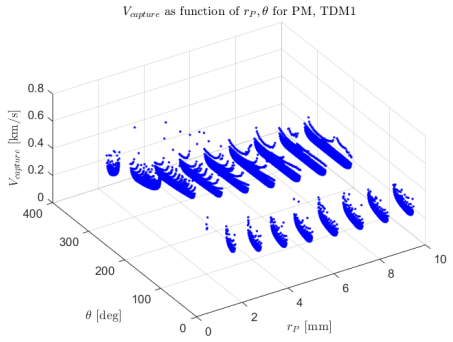

Figure 5: Capture velocity expressed as function of r_P and θ.

7. Collection Mechanism

For this work's scenario, the most suitable technology is represented by an ultra-low density silica-based aerogel capture: this technology, in fact, enables intact particle capture, preserving its elemental composition, structural phases, morphology and chemical isotopic composition. To not melt or vaporize the ejecta, aerogel slows down gradually the colliding particle by means of two layers having densities of 0.01 and 0.03 g/cm^3. Moreover, its transparency grants an easy localization and removal of captured particles. From E_{max} and literature, the thickness of aerogel panel necessary would be probably around 4 m, but other laboratory simulations are required to grant the effectiveness and efficiency of the capture. Being a passive technique, then, aerogel is simple and reliable. Concerning the collection phase, similarly to what happened in Stardust-NeXT, once in position the spacecraft shall open tennis-racket-shaped catcher filled with aerogel. Such a device shall of course be linked to a holder which, designed to maximise the exposure area, is assumed, studying past literature, to cover about the 33.84% of the surface: aiming for an exposure area of 1040 m^2 as in the case of Stardust-NeXT, the actual surface considering also the holder would be of 1392 cm^2. Summarising up, the main advantages pushing for the use of aerogel are that it is already space proven; it features high emissivity, therefore being insensitive to thermal cycles; it

is transparent, simple and reliable; being organic does not suffer of radiation or chemical erosion; being ultra-low dense no mass constraints will never arise. On the other hand, this technique has bever been used for the range of velocities found in this work but rather it is generally adopted for capture at hypervelocities (km/s): capture efficiency in these conditions still has to be proven.

8. Conclusions

This work, even though through several simplifying assumptions, successfully proved the feasibility of an on-orbit collection mission exploiting a satellite orbiting around the second libration point. Specifically, the mission will be able to gather 5.262 g of material in a time span of 23 days (excluding the travel time required to reach Ryugu's system).

References

[1] B. A. Gustafson, "Physics of zodiacal dust," *Annual Review of Earth and Planetary Sciences*, vol. 22, pp. 553–595, 1994.

[2] W. S. Koon, M. W. Lo, J. E. Marsden, and S. D. Ross, "Dynamical systems, the three-body problem and space mission design," in *Equadiff 99: (In 2 Volumes)*, pp. 1167–1181, World Scientific, 2000.

[3] S. Kikuchi, N. Ogawa, O. Mori, T. Saiki, Y. Takei, F. Terui, G. Ono, Y. Mimasu, K. Yoshikawa, S. Van Wal, *et al.*, "Ballistic deployment of the hayabusa2 artificial landmarks in the microgravity environment of ryugu," *Icarus*, vol. 358, p. 114220, 2021.

[4] M. Trisolini, C. Colombo, Y. Tsuda, *et al.*, "Ejecta dynamics around asteroids in view of in-orbit particle collection missions," in *72nd International Astronautical Congress (IAC 2021)*, pp. 1–10, 2021.

[5] A. Latino, "Ejecta orbital and bouncing dynamics around asteroid ryugu," 2019.